274 Transactions of the Korean Society of Mechanical Engineers, Vol. 8, No. 3, pp. 274~282, 1984.

<Original>

Scaling Analysis of Core Flow Pattern in a Low-Aspect Ratio Rectangular Enclosure†

——(I) Core-Driven Flow Regime——

Jinho Lee*

(Received February 28, 1984)

종횡비가 낮은 직각형 밀폐용기 내의 코어흐름 형태에 관한 해석

——(I) 운동력의 코어에 존재하는 경우——

이 진 호

초 록

밀폐용기 내의 자연대류에 의한 흐름현상에 고유하며 아직까지 해결되지 않고 있는 중요한 문제는 그 내부흐름의 형태를 주어진 물리적인 조건으로 부터 미리 예측할 수 없다는 것이다. 이는 이 문제의 해석적인 해결에 가장 큰 난점이 되고 있다.

본 논문에서는 multiple scales method를 이용한 해석적인 모델을 개발하여 종횡비가 낮은 직각형 밀폐용기 내에서 운동력이 코어에 존재하는 경우 그 내부 흐름형태를 scaling analysis를 통해 정성적으로 예측, 기존의 결과와 비교 검토하였다.

1. Introduction

1.1. General Aspect of the Problem

Natural convection in completely confined fluids occurs in many and diverse applications such as nuclear reactor systems, material processing, solar energy and environmental engineering and geophysics, and has, as a result, been receiving more attention recently. The study of natural convection flows that are completely bounded by surfaces leads to a number of diffcult problems. Natural convection is extremely sensitive to the configuration and boundary conditions. Theoretical analysis is limited because of the inherent coupling and nonlinearity of the basic equations.

Most of the earlier works were concerned with natural convection in horizontal cylinders and high aspect ratio rectangles. A comprehensive review of earlier existing works has been done by Ostrach[1]. More recent research on natural convection flows in horizontal, vertical and tilted rectangular enclosures was reviewed by Catton[2]. Despite an ever increasing amount of research on confined natural convection, a problem inherent to all situations of this type that remains unsolved is that the core flow patterns cannot be predicted a priori from the given geometry and boundary conditions. As is pointed out in(1), in the confined natural convection problems in horizontal cylinders and high aspect ratio rectangles, two core configurations are mathematically possible, viz.,

† Presented at KSME Autumn Conference, 1983

* Member, Department of Mechanical Engineering, Yonsei University.

rotating and isothermal or stagnant and stratified. Analytical and numerical solutions first indicated the former and it was only after experiments indicated that the latter always occurred and thereafter such results were obtained theoretically. Similarly in the low aspect ratio rectangular enclosures, analysis[3] showed that the core flow structure is always parallel when aspect ratio, A, goes to very small value with arbitrary but fixed value of Gr, Grashof nuwber based on cavity height, and it was indicated by experiments[4~7] and numerical works[8~11] that the flow pattern in the core is not always parallel. Under certain conditions, there appeared other types of core configurations such as secondary cells or stagnant flows in the core. Such ambiguities concerning the nature of the flows are inherent in all internal convection problems as has been shown above and no reliable analytical method, as yet, exists to predict, a priori, the core flow pattern. A primary motivation of the present work is to develop some means to predict the core flow pattern, a priori, in low aspect ratio rectangular enclosures. Emphasis is given to "heated-from-the side" configura tions, because such configurations contain all the essential physics that are common to all confined natural convection flows.

1.2. Method of Approach

In a low aspect retio ractangular enclosure, the flow region can, on a geometric basis, be divided into two regions. One, the region near end walls which we will call herein "end region" and the other, "core region", the region outside the end regions with horizontal boundaries(Fig. 1). For a given fluid and geometry, when the Rayleigh number(i.e., the temperature difference between the end walls) is small, temperature gradient will be felt across the entire configuration and thus the heat transfer between the end walls will be mainly by conduction in the core. In this situation, the primary driving force for the fluid motion will be the buoyancy force in the core. This flow regime will be called herein the "core-driven flow regime". On the other hand, when the Rayleigh number is sufficiently high the transfer of heat by conduction in the core will be negligible. Most of the temperature drop(or increase) in this situation will occur in the end regions and will be convected across the cavity to opposite end. There thus will no longer exist the driving force in the core, and instead, it will come from the end regions. This flow regime will be called the "end-driven flow regime". In between the two flow regime, it will be called the "intermediate flow regime".

In order to be able to predict the core flow pattern, and thus, the whole flow pattern correctly, one has to be clear on what physical mechanisms govern the flow. To do this, one has to develop a mathematical model which properly represents the phyics of the core flow. Since the flow characteristics may be different and coupled in each flow region, it may not be possible to consider all the important physical mechanisms in the enclosure by basic equations for either region. In addition, the equations that describe the phenomena of interest herein are nonlinear and bidirectionally coupled.

In order to ensure that an assumption made in one equation is consistently transmitted to the other equations, a formal procedure is employed herein based on the method of multiple scales, see Nayfeh[12]. Multiple scales are introduced to give mathematical degrees of freedom which enable physical statements (force or energy balance) to be properly made on the important physical mechanisms in the enclosure.

Based on a scaling analysis which gives degrees of freedom, proper physical balances in the basic dimensionless equations can be made and the order of magnitude of each physical terms can be estimated with the relevant dimensionless parameter as its coefficient. Then, by considering the derivatives with respect to the core flow region, the equations which will describe the core flow characteristics can be extracted from the basic dimensionless equations. The core flow patterns are then studied in a global sense under the implicit assumption that there exists no flow subregimes such as secondary cells. On that basis, the geometric length scales are the proper ones for the core flow structure. In the present paper, consideration is given to the core-driven flow regime

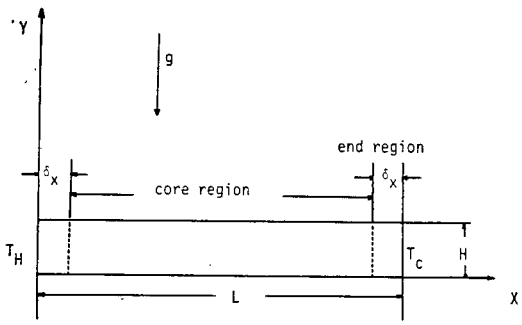

Fig. 1 Schematic diagram of the system

and leave the end-driven flow regime to the part Ⅱ of the companion paper.

2. Formulation of the Problem

The flow field to be studied herein is assumed steady, two-dimensional, laminar and quasi-incompressible. Quasi-incompressibility is generally referred to as Boussinesq approximation and has been discussed in a formal way by Ostrach[13].

2.1. Normalization of the Basic Equations

The basic equations of vorticity and energy transport for two-dimensional flow can be written as

$$\frac{\partial(\Omega, \Psi)}{\partial(X, Y)}=\beta g\frac{\partial T}{\partial X}+\nu\left(\frac{\partial^2\Omega}{\partial X^2}+\frac{\partial^2\Omega}{\partial Y^2}\right) \tag{1}$$

$$\Omega=-\left(\frac{\partial^2\Psi}{\partial X^2}+\frac{\partial^2\Psi}{\partial Y^2}\right) \tag{2}$$

$$\frac{\partial(T, \Psi)}{\partial(X, Y)}=\alpha\left(\frac{\partial^2 T}{\partial X^2}+\frac{\partial^2 T}{\partial Y^2}\right) \tag{3}$$

where Ω denotes vorticity, Ψ stream function, T temperature and $\frac{\partial(\Omega, \Psi)}{\partial(X, Y)}=\frac{\partial\Omega}{\partial X}\frac{\partial\Psi}{\partial Y}-\frac{\partial\Omega}{\partial Y}\frac{\partial\Psi}{\partial X}$. Also g is the acceleration due to gravity and ν, β and α, the kinematic viscosity, coefficient of thermal expansion and thermal diffusivity. The viscous dissipation was neglected in the energy equation (3) due mainly to the very low velocities present in natural convection flows of the type considered herein. The variations of the dynamic viscosity μ and thermal conductivity κ were also neglected as a result of the quasi-incompressibility of the fluid.

The basic equations (1)~(3) are normalized by the following definitions.

$$x=\frac{X}{L},\ y=\frac{Y}{H},\ \psi=\frac{\Psi}{\Psi_R} \tag{4}$$

$$w=\frac{\Omega}{\Omega_R}=\frac{\Omega}{\Psi_R/l^2},\ \theta=\frac{T-T_C}{T_H-T_C}$$

In (4), the characteristic stream function Ψ_R is to be specified later in the analysis in accordance with the physical situations of the problem. The characteristic vorticity Ω_R is represented as Ψ_R/l^2, where l is a length scale that will also be specified in the course of analysis. The purpose of introducing the unspecified length scale l (instead of using the specific geometry length scale) is to normalize the vorticity properly according to the physics of the system.

Substitution of the definition(4) into Eqs. (1)~(3) yields

$$\frac{\partial(w, \psi)}{\partial(x, y)}=\frac{\beta g\Delta T H l^2}{\Psi_R^2}\frac{\partial\theta}{\partial x}+\frac{\nu L}{\Psi_R H}\left(A^2\frac{\partial^2 w}{\partial x^2}+\frac{\partial^2 w}{\partial y^2}\right) \tag{5}$$

$$w=-\frac{l^2}{H^2}\left(A^2\frac{\partial^2\psi}{\partial x^2}+\frac{\partial^2\psi}{\partial y^2}\right) \tag{6}$$

$$\frac{\partial(\theta, \psi)}{\partial(x, y)}=\frac{\alpha L}{\Psi_R H}\left(A^2\frac{\partial^2\theta}{\partial x^2}+\frac{\partial^2\theta}{\partial y^2}\right) \tag{7}$$

where $\Delta T=T_H-T_C$ and A represents the aspect ratio, $\frac{H}{L}$

Referring to Fig. 1, the corresponding boundary conditions become

$$\psi=\frac{\partial\psi}{\partial x}=0,\ \theta=1,\ 0 \text{ at } x=0,\ 1 \tag{8a}$$

$$\psi=\frac{\partial\psi}{\partial y}=0,\ \frac{\partial\theta}{\partial y}=0 \text{ at } y=0,\ 1 \tag{8b}$$

And by the centro-symmetry property of the equations and boundary conditions[14],

$$\psi(x, y)=\psi(1-x, 1-y) \tag{9a}$$

$$\theta(x, y)=1-\theta(1-x, 1-y) \tag{9b}$$

2.2. Working Form of the Equations

In the dimensionless equations (5)~(7), when $A^2 \ll 1$ the x-direction diffusions terms can be neglected compared to the y-direction diffusion terms. Since the x-direction diffusion terms are the highest order x-derivatives, if they are neglected, the end wall boundary conditions can not be fully satisfied. Therefore, the equations without the horizontal diffusion terms in Eqs. (5)~(7) are only valid away from the ends, i.e., in the core. Instead, the equations which represent the flow characteristics in the end

regions could be obtained by properly stretching the x-coordinate in Eqs. (5)~(7).

In order to obtain insights into the nature of flow charactics, the unspecified characteristic quantities such as $\mathcal{V}_R$ and l in Eqs. (5)~(7) should be determined first to see what the relevant dimensionless parameters are. These quantities may, in principle, be determined by considering the flow mechanisms in either region. However, as the two regions are closely coupled and this coupling affects much of the flow structure, it is necessary that in determining the characteristic quantities both flow regions and their coupling be considered in some way. Otherwise, important physical mechanisms may be overlooked. A mathematically formal procedure is, therefore, employed on the basis of the method of multiple scales through which both the end core flow regions together with the interacting region are explicitly identified in the basic dimensionless equations.

Here the physical domain of interest is confined and finite and the singular behaviour of the dimensionless equations are expected near the end walls. Thus the multiple scales are introduced in the following way (see, 12).

$$\zeta=x,\quad \eta=\frac{x}{\varepsilon_x} \tag{10}$$

The derivatives are

$$\frac{\partial}{\partial x}=\frac{1}{\varepsilon_x}\frac{\partial}{\partial \eta}+\frac{\partial}{\partial \zeta}$$

$$\frac{\partial^2}{\partial x^2}=\frac{1}{\varepsilon_x^2}\frac{\partial^2}{\partial \eta^2}+\frac{2}{\varepsilon_x}\frac{\partial^2}{\partial \eta \partial \zeta}+\frac{\partial^2}{\partial \zeta^2} \tag{11}$$

where the derivatives with resdect to ζ and η represent the core and end region characteristics, respectively, and ε_x is a small, stretching parameter defined as

$$\varepsilon_x=\frac{\delta_x}{L} \tag{12}$$

where δ_x is the end region characteristic length scale.

Introducing the derivatives of the multiple scales (12) into the dimensionless equations (5)~(7), we then obtain

$$\frac{1}{\varepsilon_x}\frac{\partial(w,\psi)}{\partial(\eta,y)}+\frac{\partial(w,\psi)}{\partial(\zeta,y)}=\frac{\beta g \Delta T l^2 H}{\mathcal{V}_R^2}\left(\frac{1}{\varepsilon_x}\frac{\partial\theta}{\partial\eta}+\frac{\partial\theta}{\partial\zeta}\right)+\frac{\nu L}{\mathcal{V}_R H}\left(\frac{A^2}{\varepsilon_x^2}\frac{\partial^2 w}{\partial\eta^2}+2\frac{A^2}{\varepsilon_x}\frac{\partial^2 w}{\partial\eta\partial\zeta}+A^2\frac{\partial^2 w}{\partial\zeta^2}+\frac{\partial^2 w}{\partial y^2}\right) \tag{13}$$

$$w=-\frac{l^2}{H^2}\left(\frac{A^2}{\varepsilon_x^2}\frac{\partial^2\psi}{\partial\eta^2}+2\frac{A^2}{\varepsilon_x^2}\frac{\partial^2\psi}{\partial\eta\partial\zeta}+A^2\frac{\partial^2\psi}{\partial\zeta^2}+\frac{\partial^2\psi}{\partial y^2}\right) \tag{14}$$

$$\frac{1}{\varepsilon_x}\frac{\partial(\theta,\psi)}{\partial(\eta,y)}+\frac{\partial(\theta,\psi)}{\partial(\zeta,y)}=\frac{\alpha L}{\mathcal{V}_R H}\left(\frac{A^2}{\varepsilon_x^2}\frac{\partial^2\theta}{\partial\eta^2}+2\frac{A^2}{\varepsilon_x^2}\frac{\partial^2\theta}{\partial\eta\partial\zeta}+A^2\frac{\partial^2\theta}{\partial\zeta^2}+\frac{\partial^2\theta}{\partial y^2}\right) \tag{15}$$

These are the working form of the basic dimensionless equations.

In the following analysis, the dimensionless groups are to be determined by proper physical balances in Eqs. (13)~(15). Then the core flow characteristics are going to be studied from a global view by noting the character of the dimensionless groups, then observing their effects on the equations as they are allowed to take on limiting values.

3. Global Core Configuration

The driving force of the fluid motion in the core-driven flow regime is the buoyancy force induced primarily by the temperature gradient in the core. We thus study the core configuration first considering the balance between the buoyancy and viscous forces implying that the viscous effect is dominant in the core compared to the inertia effect, and then that between the buoyancy and inertia forces which implies that the inertia effect is dominant in the core. The explicit conditions for each situation will be delineated in the course of analysis.

3.1. Viscous-Effect Dominated Core

(A) Core Flow Equation

From Eq(13), the balance between buoyancy and viscous forces in the core can be represented as

$$\frac{\beta g \Delta T l^2 H}{\mathcal{V}_R^2}\sim\frac{\nu L}{\mathcal{V}_R H} \tag{16}$$

Considering that the buoyancy force in the core drives the core flow and that there is not supposed to exist any particular region in the core flow, it is appropriate to represent the characteristic vorticity Ω_R by specifying the characteristic length l by H, as

$$Q_R=\frac{\Psi_R}{H^2} \tag{17}$$

From (16) and (17), we obtain (17)

$$\Psi_R\sim\frac{\beta g\Delta TH^4}{\nu L} \tag{18}$$

One more balance is required to determine the stretching parameter, ε_x, from which the end region flow equations and its characteristic length scale can be determined. However, at this moment, that is not clear before we know the physics of core flow. Thus, we leave the determination of ε_x to later section.

Substituting (18) into Eqs. (13)~(15) and considering the terms with ζ and y derivatives, the equations which will describe the core flow characteristics can be written as

$$Gr\,A^2\frac{\partial(w,\psi)}{\partial(\zeta,y)}=\frac{\partial\theta}{\partial\zeta}+A^2\frac{\partial^2 w}{\partial\zeta^2}+\frac{\partial^2 w}{\partial y^2} \tag{19}$$

$$w=-\left(A^2\frac{\partial^2\psi}{\partial\zeta^2}+\frac{\partial^2\psi}{\partial y^2}\right) \tag{20}$$

$$PrGr\,A^2\frac{\partial(\theta,\psi)}{\partial(\zeta,y)}=A^2\frac{\partial^2\theta}{\partial\zeta^2}+\frac{\partial^2\theta}{\partial y^2} \tag{21}$$

For the situation described above, it is now evident that our analysis is valid under the condition $GrA^2\leq 1$. Beyond this condition, i.e., for $GrA^2\gg 1$, inertia effect becomes dominant in the core, and thus, different scalings are required based on different force balances for the analysis of that situation.

(B) Core Flow Characteristics

(1) $GrA^2\ll 1$, $A^2\ll 1$

Since Pr appears as a parameter in Eq. (21), its effect must be analyzed.

(i) $Pr\lesssim 1\rightarrow RaA^2\ll 1$

When $Pr\leq 1$ such that $RaA^2\ll 1$, Eq. (21) may reduce to

$$0=\frac{\partial^2\theta}{\partial y^2} \tag{22}$$

Considering the adiabatic horizontal boundary conditions (8b). the heat flow is one-dimensional in a purely conductive regime. θ thus can be represented as

$$\theta=\theta(\zeta)=K_1\zeta+K_2 \tag{23}$$

where K_1, K_2 are arbitrary constants to be determined from the matching with the end region solutions.

From Eqs. (19), (20) and (23) with the corresponding boundary conditions in(8), we can obtain

$$\psi=\frac{K_1}{24}y^2(y-1)^2 \tag{24}$$

which represents the parallel core flow pattern.

(ii) $Pr\gg 1\rightarrow RaA^2\sim 1$

When Pr is large such that $RaA^2\sim 1$, Eq. (21) may reduce to

$$\frac{\partial(\theta,\psi)}{\partial(\zeta,y)}=\frac{\partial^2\theta}{\partial y^2} \tag{25}$$

Rewriting Eq. (25) and integrating with respect to y from $y=0$ to 1, we have

$$\int_0^1\left[\frac{\partial}{\partial\zeta}\left(\theta\frac{\partial\psi}{\partial\zeta}\right)+\frac{\partial}{\partial y}\left(-\theta\frac{\partial\psi}{\partial\zeta}-\frac{\partial\theta}{\partial y}\right)\right]dy=0 \tag{26}$$

By changing the order of integration and diffrentiation and applying the Leibnitz's rule, Eq. (26) can be rewritten as

$$\frac{\partial}{\partial\zeta}\int_0^1\theta\frac{\partial\psi}{\partial y}dy=\frac{\partial}{\partial y}\int_0^1\left(\theta\frac{\partial\psi}{\partial\zeta}+\frac{\partial\theta}{\partial y}\right)dy \tag{27}$$

Integrating the left hand side by parts and applying the boundary conditions(8), we finally have

$$\frac{\partial}{\partial\zeta}\int_0^1\psi\frac{\partial\theta}{\partial y}dy=0 \tag{28}$$

It can be shown (see, 15) that the only possible core configuration which can satisfy the Eq. (28) is

$$\theta=K_3\zeta+g(y) \tag{29a}$$

and

$$\psi=K_3\,h(y) \tag{29b}$$

where K_3 is an arbitrary constant and $g(y)$, $h(y)$ are an arbitary function of y. Eq. (29) represents that the temperature distribution in the core is linear and stratified while the corresponding core flow pattern is parallel.

From Eqs. (19), (20) and (29) with the corresponding boundary conditions of (8), $h(y)$ can be represented as

$$h(y)=\frac{1}{24}y^2(y-1)^2 \tag{30}$$

(2) $Gr\,A^2\sim 1$, $A^2\ll 1$

(i) $Pr\ll 1\rightarrow Ra\,A^2\ll 1$

When Pr is very small such that $RaA^2\ll 1$, Eq. (21) reduces to the same form as Eq. (22) which was previously treated. Referring the result of (23), θ can be represented as

$$\theta=K_1\zeta+K_2 \tag{31}$$

Under the present condition the flow characteristics from Eq. (19) is not readily perceivable due to its nonlinearity. We thus try to get information from

an integral from of Eq. (19) as we did with Eq. (25) in the preceding analysis.

If we rewrite and integrate Eq. (19) over y from 0 to 1, for $GrA^2 \sim 1$ we have

$$\frac{\partial}{\partial \zeta}\int_0^1 w\frac{\partial \psi}{\partial y}dy+\frac{\partial}{\partial y}\int_0^1\left(-w\frac{\partial \psi}{\zeta \partial}-\frac{\partial w}{\partial y}\right)dy = \int_0^1 \frac{\partial \theta}{\partial \zeta}dy \tag{32}$$

Substituting the vorticity equation (20) and the linear temperature profile (31) into Eq. (32), and applying the proper boundary conditions, we then have

$$\frac{\partial}{\partial \zeta}\int_0^1 \psi\frac{\partial^3 \psi}{\partial y^3}dy+\frac{\partial^3 \psi}{\partial y^3}\Big|_0^1 = K_1 \tag{33}$$

Considering the boundary condition, ψ can be represented as

$$\psi(\zeta, y)=f(\zeta)g(y) \tag{34}$$

where $f(\zeta)$, $g(y)$ is an arbitrary function of ζ and y, respectively. Substituting(34) into Eq. (33) and carrying out the differentiation, we find

$$2f(\zeta)f'(\zeta)\int_0^1 g(y)g'''(y)dy+f(\zeta)[g'''(y)|_0^1] = K_1 \tag{35}$$

From the symmetry property of ψ in(9), the function $g(y)$ is an even function about the point $y=1/2$. Then the product $g(y)\ g'''(y)$ is an odd function about $y=1/2$, and the integral $\int_0^1 g(y)g'''(y)dy$ becomes zero. Eq. (35) thus reduces to

$$f(\zeta)[g'''(y)|_0^1]=K_1 \tag{36}$$

This gives

$$f(\zeta)=\frac{K_1}{[g'''(y)|_0^1]}=\text{const.}=K_4 \tag{37}$$

Then from Eqs. (34) and (37).

$$\psi=K_4 g(y) \tag{38}$$

which shows the parallel core flow structure.

From Eqs. (19), (20) and (38) with the proper boundary conditions, $g(y)$ can be given as

$$g(y)=\frac{K_1}{K_4}\frac{1}{24}y^2(y-1)^2 \tag{39}$$

(ii) $Pr \sim 1 \rightarrow Ra\,A^2 \sim 1$

When Pr is of order 1 such that $Ra\,A^2 \sim 1$, Eq. (21) reduces to the same from as Eq(25). By the similar procedure as in the preceding analysis, ψ and θ can be represented as

$$\psi=\psi(y) \tag{40}$$

and

$$\theta=f(\zeta)+g(y) \tag{41}$$

Substituting Eqs. (40), (41) and (20) into Eq. (19) and for $GrA^2 \sim 1$ applying the proper boundary conditions, θ and ψ canbe given as

$$\theta=K_5\zeta+g(y) \tag{42}$$

and

$$\psi=\frac{K_5}{24}y^2(y-1)^2 \tag{43}$$

where K_5 is an arbitrary constant. Eqs. (42) and (43) show that the core flow pattern is still parallel while the core temperature distribution is linear and stratified.

(iii) $Pr \gg 1 \rightarrow RaA^2 \gg 1$

When Pr is large such that $RaA^2 \gg 1$, from Eq. (21) the heat transfer by conduction is negligible and convection becomes dominant in the core. There thus no longer exists the driving force in the core. Instead the driving force will come out from the end region. This corresponds to the end-driven flow regime and will be considered in Part II, the companion paper.

(3) $GrA^2 \gg 1$, $A^2 \ll 1$

Under this condition, from Eq. (19) inertia becomes dominant in the core. Thus the force balance balance made on the basis of viscous-effect dominated core becomes inappropriate. This situation will be treated in the case of inertia-effect dominated core.

(c) Determination of Stretching Parameter, ε_x

In the preceding analysis, it was shown that in the viscous-effect dominated core the temperature distribution in the core is either linear or linear and stratified and the core flow structure is parallel. In such a flow regime, the end regions are supposed to have little effect on the core flow except that they simply turn the core flow to conserve the mass. Then the proper physical balance in the end region that is needed to determine ε_x could be that between the viscous diffusion along the end walls and that along the horizontal boundaries in the end region. From Eq. (13), this balance can be represented as

$$\frac{A^2}{\varepsilon_x^2}\sim 1 \tag{44}$$

and thus $\varepsilon_x \sim A$ (45)

From (12) and (45), the end region characteristic length, δ_x, is given as

$$\delta_x = \varepsilon_x \cdot L \sim H \tag{46}$$

It is thus seen from (46) that the end regions penetrate a distance of order H into the core. In other words, the core configurtions obtained above are thought to be valid outside a distance of order H from the either end.

The predicted core configurations in the above analysis show excellent agreement with those of Cormack et. al's asymptotic theory[3] except the validity criterion. While the present analysis simply gives $RaA^2 \leq 1$ for its validity, Cormack et. al's approximate criterion is $Ra^2A^3 \leq 10^5$. In addition, the present analysis gives the proper physical meaning of the characteristic stream function and the end region characteristic length scale which were used in cormack et. al's work without any justification. It is very important to know accurately the physical meaning of the characteristic quantities defined in the analysis, because in many cases they give the proper physical conditions within which the analysis is valid.

3.2. Inertia-Effect Dominated Core

(A) Core Flow Equations

It was shown in the previous analysis that the balance between the buoyancy and viscous forces made therein becomes inappropriate when $GrA^2 \gg 1$, because the ineria effect becomes dominant under that condition. We now study the flow characteristics of this situation considering the balance between the buoyancy and inertia forces in the core.

From Eq. (13), the balance between the buoyancy and inertia forces in the core can be represented as

$$\frac{\beta g \Delta T l^2 H}{\Psi_R^2} \sim 1 \tag{47}$$

Specifying l as H by the same reasoning in (17), Ψ_R becomes

$$\Psi_R \sim (\beta g \Delta T H^3)^{1/2} \tag{48}$$

Here we also leave the determination of the stretching parameter ε_x to later. Substituting (48) into Eqs. (13)-(15) and considering the terms with ζ and y derivatives, the core flow equationscan be written as

$$\frac{\partial(w, \psi)}{\partial(\zeta, y)} = -\frac{\partial \theta}{\partial \zeta} + \frac{1}{\sqrt{GrA^2}}\left(A^2 \frac{\partial^2 w}{\partial \zeta^2} + \frac{\partial^2 w}{\partial y^2}\right) \tag{49}$$

$$w = -\left(A^2 \frac{\partial^2 \psi}{\partial \zeta^2} + \frac{\partial^2 \psi}{\partial y^2}\right) \tag{50}$$

$$\frac{\partial(\theta, \psi)}{\partial(\zeta, y)} = \frac{1}{\sqrt{Pr^2 GrA^2}}\left(A^2 \frac{\partial^2 \theta}{\partial \zeta^2} + \frac{\partial^2 \theta}{\partial y^2}\right) \tag{51}$$

For $GrA^2 \gg 1$, Pr appears as a parameter in Eq. (51). Because consideration is being given to the situation in which the driving force exists in the core, the analysis will be valid within the parametric range of $Pr^2 GrA^2 \leq 1$ which is possible only for $Pr^2 \leq \frac{1}{GrA^2}$, i.e., for low Pr. One thing to be noted is that for $GrA^2 \gg 1$, viscous diffusion terms seem to be neglible compared to the other terms in Eq. (49). However, since these terms are the derivatives of the highest order in the equations Eq. (49) becomes singular for $GrA^2 \gg 1$ which implies that for negligible horizontal diffusion term, $A^2 \frac{\partial^2 w}{\partial \zeta^2}$, in the core for $A^2 \ll 1$, there exists a thin viscous layer very near the horizontal boundaries in which the vertical diffusion term, $\frac{\partial^2 w}{\partial y^2}$, is important.

(B) Core Flow Characteristics

(1) $Pr^2 \ll \frac{1}{GrA^2}$, $A^2 \ll 1$

When Pr^2 is very small such that $Pr^2 GrA^2 \ll 1$, fron Eq. (51) the heat transfer in the core is purely diffusive and, as treated before, θ can be given as

$$\theta = K_1 \zeta + K_2 \tag{52}$$

Then, from Eqs. (49) and(52), for $GrA^2 \gg 1$

$$\frac{\partial(w, \psi)}{\partial(\zeta, y)} = K_1 \tag{53}$$

This equation is very difficult to treat analytically. However, in order that Eq. (53) be valid, ψ should at least be a function of both variables as

$$\psi = \psi(\zeta, y) \tag{54}$$

This implies that the core flow pattern(to be accurate, the flow pattern outside the thin viscous layer near the horisontal boundaries in the core) becomes non-parallel when the inertia is important in the core, although the flow is driven by the buoyancy force in the core. This is in contradistinction to the result of Cormack et. al's asymptotic result of parallel flow Existing numerical works[10,11] do not report any non-parallel core flow structure within the present parametric range. No experimental data are available,as yet, for direct

comparision for the present configuration. This discrepancy thusneeds urgent verification.

(2) $Pr^2GrA^2\sim1$, $A^2\ll1$

Under this condition, Eq. (51) reduces to the same form as Eq. (25) which was treated before. Following the same procedure, we have the identical intergal form, Eq. (28). For the present case, however, no situation could be found in which the driving force could occur in the core(see, 15). Thus the balance based on the driving force in the core is inappropriate and the analysis based on this balance is valid only for $Pr^2GrA^2\ll1$. Actually for $GrA^2\gg1$, the condition $Pr^2Gr^2\sim1$ is possible only when $RaA^2\gg1$ for low Pr in which case the driving force exists in the end region as mentioned earlier. The condition $Pr^2GrA^2\gg1$ also corresponds to the case $RaA^2\gg1$ which will be considered in Part II.

(c) Determination of Stretching Parameter

In the above, although the core flow is driven by the buoyancy force in the core, the core flow pattern was shown to be non-parallel. In this situation, the proper force balance for the end region, from which the stretching parameter, ε_x, is determined, is not readily apparent. However, considering the relative dominance of inertia with respect to viscous friction in the core and the consequent non-parallel core flow structure, it can be inferred that the inretia in the end region can be as influential on the core flow structure as the inertia in the core. Based on this inferrence, the balance between the inertia in the end and the inertia in the core seems to be appropriate to the present situation. From Eq. (13), this balance can be represented as

$$\frac{1}{\varepsilon_x}\sim1 \tag{55}$$

and thus

$$\varepsilon_x\sim1 \tag{56}$$

From (12) and(56), δ_x becomes of order

$$\delta_x=\varepsilon_x\cdot L\sim L \tag{57}$$

This tells us that there is no difference in horizontal length scale between the core and end region, which means that no clear distinction could be made between the two regions. In addition, since $\varepsilon_x\sim1$, there is no distinction between the equations with the variables(η, y) and (ζ, y), i.e., in the end and core regions. The core flow picture in this situation will thus be valid throughout the whole cavity except the thin layer adjacent to the horizontal boundaries which is supposed to exist due to the singular behaviour of the viscous diffusion terms for $GrA^2\gg1$ in Eq. (49). Consequently the turning flow in the cavity is not necessarily confined to the region near the end walls in this case as in the case of parallel core flow. Instead it may spread over the entire configuration.

4. Summary and Concluding Remarks

Consideration has been given to the prediction of global core flow pattern through scaling analysis in the core-driven flow regime in a low aspect ratio rectangular enciosure.

In the case of viscous-effect dominated core, the balance was made between the buoyancy and viscous forces in the core. The analysis based on this balance is valid within the parametric range of $GrA^2\leq1$ and $RaA^2\leq1$. In this case, the core flow structure is parallel and the core temperature distribution is either purely linear or linear and stratified. Such core configuration was shown to be valid outside a distance of order H from either end.

In the inertia-effect dominated core, the analysis is based on the balance between the buoyancy and inertia forces in the core. The validity of analysis is limited to the parametric ranges of $G_rA^2\gg1$ but $Pr^2GrA^2\ll1$, which is only possible for low Pr. The core flow pattern was shown to be non-parallel although the core temperature profile is strictly linear. No clear distinction in the flow characteristics is thought to exist between the end and core region in this case.

By comparison, the prediction of core configuration is satisfactory in the case of viscous-effect dominated core. For the inertia-effect dominated core, experiment is urgently needed to clarify the inconsistency between the present prediction and others' results.

References

(1) Ostrach, S., "Natural Convection in Enclosures", in Advances in Heat Transfer, Vol.8, pp. 161~226, Academic Press, New York, 1972

(2) Catton, I., "Natural Convection in Enclosures", Proc. 6th Heat Transfor Conference, Vol.1. pp. 13~31, 1978

(3) Cormack, D.E., Leal, L.G. and Seinfeld, J.H., "Natural Convection in a Shallow Cavity with Differentially Heated End Walls. Part 1. Asymptotic Theory", J. Fluid Mech., Vol. 65, pp. 209~229, 1974

(4) Imberger, J., "Natural Convection in a Shallow Cavity with Differentially Headed End Walls. Part 3. Experimental Results", J. Fluid Mech., Vol. 65, pp. 247~260, 1974

(5) Al-Homoud, A.A., "Experimental Study of High Rayleigh Number Convection in Horizontal Cavity with Different End Temperatures", M.S. Thesis, Univ. of Colorado, Boulder, Colorado, 1979

(6) Ostrach, S, Loka, R.R. and Kumar, A., "Natural Convection in Enclosures", edit. by Torrance and Catton, ASME HTD-Vol. 18, 1980

(7) Kamotani, Y., Wang, L.W. and Ostrach, S., "Experiments on Natural Convection Heat Transfer in Low Aspect Ratio Enclosures", AIAA Journal, Vol. 21, pp. 200~294, 1983.

(8) Cormack, D.E., Leal, L.G. and Seinfeld, J.H., "Natural Convection in a Shallow Cavity with Differentially Heated End Walls Part 2. Numerical Solutions", J. Fluid Mech., Vol. 65, pp. 231~246, 1974

(9) Lee, E.I. and Sernas, V., "Numerical Study of Heat Transfer in Rectangular Air Enclosures of Aspect Ratio Less Than One", ASME Paper 80-WA/HT-43, 1980

(10) Shiralkar, G.S. and Tien, C.L., "A Numerical Study of Laminar Natual Convection in Shallow Cavities", J. Heat Transfer, Vol. 103, pp. 226~231, 1981

(11) Hart, J.E. "Low Prandtl Number Convection Between Differentially Heated End Walls", Int. J. Heat Mass Transfer, Vol. 25, pp. 1069~1074, 1983

(12) Nayfeh, A., "Perturbation Methods", Chap. 6, pp. 228~307, John Wiley and Sons, New York, 1973

(13) Ostrach, S., "Laminar Flows with Body Forces", in High Speed Aerodynamics and Jet Propulsion (F,K, Moore, edit), Vol. 4, Chap.F, Princeton Univ. Press, Princeton, New Jersy 1964

(14) Gill, A.E., "The Boundary-Layer Regime for Convection in a Rectangular Cavity," J. Fluid Mech., Vol. 26, pp. 515~536, 1966

(15) LEE, J. and Ostrach, S., "Prediction of Natural Convection Flow Pattern in Low-Aspect Ratio Enclosures", FTAS/TR-82—158, Case Western Reserve Univ., Cleveland, Ohio, 1982